An analysis of $\gamma p \rightarrow \pi^+\pi^+\pi^-n$ at 6 GeV using CLAS at Jefferson Lab

Prospectus of Dissertation

Craig Bookwalter

Department of Physics, Florida State University

August 20, 2008

Major professor: _____

Committee member: _____

Committee member: _____

Committee member: _____

Committee member: _____

1 Introduction

1.1 Theoretical Development

In the early 1960s, the search for the elementary constituents of matter was at an impasse. Physicists, expecting to find a small number of elementary particles making up protons and neutrons, were in fact finding an extraordinary number of unique particles in their scattering experiments. Several attempts to organize the melange of new particles failed until Gell-Mann, Zweig, and Ne'eman each independently proposed the quark model [1].

The quark model (in its original form) claims that all hadrons can be built from two or three quarks, of which there are three different flavors; up, down, and strange (u, d, and s). The quark model assumes an underlying symmetry which can be described mathematically by group theory, specifically as a special unitary group in three dimensions (the group of all three-by-three unitary matrices with determinant equal to one). We label this group as $SU(3)_F$, with F to remind us that flavor is the the symmetric property. Constructing the meson and baryon spectra then becomes a matter of coupling two (meson) or three (baryon) $SU(3)_F$ objects (quarks) according to rules similar to those used for coupling angular momenta (which obeys the rules of $SU(2)$). The relevant results are as follows:

$$3 \otimes \bar{3} = 1 \oplus 8 \tag{1}$$

$$3 \otimes 3 \otimes 3 = 1 \oplus 8 \oplus 8 \oplus 10 \tag{2}$$

Equation 1 states that a quark and an antiquark will combine into a flavor singlet and a flavor octet. There is an $8 \oplus 1$ object for each meson spin-parity, or J^P combination. Also, Equation 2 states that three quarks will combine into a flavor singlet, two flavor octets and one flavor decuplet.

On the basis of $SU(3)_F$, in 1962, Gell-Mann predicted the existence of an as-yet unseen baryon, the Ω^- (sss), at a mass of 1680 MeV/c^2[1]. Two years later the Ω^- was observed during experiments at Brookhaven National Laboratory [2].

However, even as Gell-Mann's successful prediction made a powerful case for the quark model, unexplained difficulties remained. If $SU(3)_F$ was an exact symmetry of nature, it would allow for the exchange of any two flavors of quark without any change in mass. Examining the masses of the members of any $SU(3)_F$ multiplet, one finds that the masses are not all equal, a sign that $SU(3)_F$ symmetry is broken by Nature. Instead there is a trend

where mass is proportional to strangeness, and we now estimate the strange quark mass to be on the order of ten times as massive as the up- and down-quarks. Thus Nature does not strictly obey $SU(3)_F$, and possiblities arise for the existence of a more fundamental symmetry.

Another quark model mystery was the existence of the doubly-charged Δ^{++}. The Δ^{++} is supposedly a bound state of three up-quarks, with all three spins aligned, but that leaves three fermions in the same quantum state, which violates the Pauli exclusion principle.

Also, in 1970, Glashow, Iliopoulos and Maiani postulated the existence of a fourth quark (called "charm" or c-quark) to explain weak interactions [4], which renders the three-dimensional symmetry of $SU(3)_F$ incomplete. Their prediction was confirmed in 1974 by the simultaneous discovery of the J/ψ charmed meson at Brookhaven [5] and at the Stanford Linear Accelerator Center (SLAC) [6]. Thus the quark model as conceived by Gell-Mann, Zweig, and Ne'eman was proven to be insufficient.

However, Gell-Mann was already responsding to these questions. With Fritzsch, he proposed a new symmetry [3] upon which to describe quark-level interactions, based on what came to be called color charge. Color charge was postulated to be an additional quantum number possessed by each quark. It takes on three values and also obeys the rules of $SU(3)$. The color force is mediated by way of eight spin-1 gauge bosons known as gluons. Unlike photons, gluons can self-interact, which causes the color force to increase as two quarks are separated. As the energy stored in the gluon field between two quarks approaches the rest mass of a new quark-antiquark pair, the field snaps and two new hadrons are created. This explains why we have never directly observed quarks, gluons, or the color charge in experiments; they are always encapsulated within hadrons. In addition, there is no such thing as a color multiplet, like the octets and decuplets of the early quark model. Every resonance we observe in nature is in a color singlet state.

This new theory of color, or quantum chromodynamics (QCD) as it came to be called, has become our best theory for predicting meson and baryon spectra. QCD spectra are much richer than that of the quark model; hadrons are no longer restricted to just $q\bar{q}$ or qqq states. States of four or five quarks or more are theoretically possible, as are states with valence gluons, or states composed entirely of glue (glueballs). The experimental search for these non-$q\bar{q}$ (exotic or hybrid) mesons is the thrust of this prospectus.

Exotic mesons were postulated even before the birth of QCD. In 1968, Rosner [7] noted that an attempt to map the finite-energy sum rule description of direct-channel resonances into Regge phenomenology was largely successful, with the only exception being states decaying to a baryon-antibaryon pair . He resolved the disconnect by postulating

the existence of mesons with quantum numbers inconsistent with those permitted by the quark model–the first exotic mesons. However, his work received little or no attention from his experimentalist contemporaries.

One of the first widely successful models in the QCD era is the MIT bag model. First proposed in 1974 by Chodos and collaborators [8], the bag model treats hadronic matter as groups of massless particles that are confined within a bag. The equilibrium radius is thus determined by the equilibrium between external pressure on the bag and the internal kinetic pressure of the quarks. Theorists quickly and copiously expanded on the work in [8] to study bag model predictions for non-$q\bar{q}$ mesons, beginning with the work of Jaffe on tetraquarks [9] and Barnes and collaborators on glueballs and $q\bar{q}g$ hybrids [10], [11].

However, the seminal work characterizing exotic mesons was published in 1982 by Isgur and Paton [12]. Their model discards the bag-model prescription of a constituent gluon to accompany the quarks, instead treating the hadron system as being built of quarks and flux-tubes. The concept has its root in lattice QCD, where spacetime is discretized into a grid, and quarks are located at the vertices of the grid and gluons are the lines connecting the vertices. In the simplest case, a quark-antiquark pair is connected by a flux tube in the ground state, and the resulting meson is an ordinary quark-antiquark pair. But inducing a vibration in the flux tube increases the total angular momentum, leading to states with quantum numbers which may lie outside those predicted by the quark model. The quantum numbers conventionally used in light (u, d, and s) meson spectroscopy are the total angular momentum J, the parity P, and the charge conjugation parity C. In order to calculate the J^{PC} allowed by the quark model for a given system, the following prescription must be applied:

$$J = L + S \tag{3}$$

$$P = (-1)^{L+1} \tag{4}$$

$$C = (-1)^{L+S} \tag{5}$$

where L is the orbital angular momentum between the decay particles and S is the coupled individual spins of the decay particles. This procedure delivers the allowed quantum numbers for a quark-model state: $J^{PC}(QM) = 0^{-+}, 1^{--}, 2^{-+}, 3^{--}...$ and so on. Any state found to have different quantum numbers is defined as exotic.

Thus, it is an important test of QCD to search experimentally for evidence of these states that are not accounted for in the quark model. In the context of the flux-tube model, it is practical to hunt for particles with non-quark-model quantum numbers, even though non-$q\bar{q}$ mesons with quantum numbers indistinguishable from ordinary

mesons are also predicted to exist [13]. Such particles can be detected experimentally, but only by other signatures such as unusual decay channels. Several collaborations have performed experiments in search of exotics, and their results are summarized in the next section.

2 Identifying Meson Resonances

In 1909, Ernest Rutherford performed the first nuclear physics experiment when he scattered alpha particles off of gold foil. From examining the angular distribution of the scattered alpha particles, he determined that the positive charge of the atom was concentrated in a small volume in the center called the atomic nucleus. Since he was interested in testing J.J. Thomson's plum-pudding model of the atom, Rutherford connected this angular distribution to the cross-sectional area of the scattering center:

$$\frac{d\sigma}{d\Omega} = \left(\frac{\alpha\hbar c}{2mv_0^2}\right)^2 \frac{1}{sin^4(\theta/2)} = \mathcal{I}(\theta) \tag{6}$$

Integrating $d\sigma$ over the entire angular range $d\Omega$, Rutherford was able to ascertain that the charge of the gold atom was concentrated in a small volume in the center: the atomic nucleus.

Nearly a hundred years later, the differential cross-section is still one of the most important quantities in scattering experiments. Traditional discovery experiments rely on observing new peaks in relevant mass spectra, but the states we are looking for are often broad and hidden beneath mass signals for other nonexotic mesons with the same kinematics. Thus, we use partial wave analysis to separate out individual states that when added together produce the total observed mass and intensity distributions.

To understand how partial wave analysis works, it is instructive to consider the case of a nonrelativistic spinless particle interacting with a central potential. To begin, we can solve the three-dimensional Schrödinger equation for the region outside of the effective range of the potential. The general solution for this region is:

$$\psi(r,\theta,\phi) = A\left[e^{ikz} + \sum_{l,m} C_{l,m} h_l^{(1)}(kr) Y_{lm}(\theta,\phi)\right] \tag{7}$$

$$= A\left[e^{ikz} + k\sum_{l=0}^{\infty} i^{l+1}(2l+1) a_l h_l^{(1)}(kr) P_l(cos\theta)\right] \tag{8}$$

where the ϕ dependence is removed by assuming a central potential. The e^{ikz} term represents the incoming plane

wave, and the second term represents an outgoing spherical wave that is an infinite sum of the product of spherical Hankel functions $h_l^{(1)}(kr)$ and Legendre polynomials $P_l(cos\theta)$, each with a corresponding partial-wave amplitude a_l. In the limit of large r, the spherical Hankel functions behave like $(-i)^{l+1}\frac{e^{ikr}}{kr}$, which leaves

$$\psi(r,\theta) \approx A\left[e^{ikz} + f(\theta)\frac{e^{ikr}}{kr}\right] \tag{9}$$

with

$$f(\theta) = \sum_{l=0}^{\infty}(2l+1)a_l P_l(cos\theta) \tag{10}$$

and furthermore,

$$|f(\theta)|^2 = \mathcal{I}(\theta,\phi) \tag{11}$$

Equation 10 is the original equation of partial wave analysis. The amplitudes a_l determine "how much" of each l-wave is in the observed intensity distribution.

For relativistic particles with spin scattering from an arbitrary potential, the procedure is more complicated. We expand the intensity distribution $\mathcal{I}(\tau)$ (where τ is a function of all of the relevant kinematical variables, such as the angles θ and ϕ, momentum transfer t, etc) in terms of decay amplitudes $A_\alpha(\tau)$ that we can calculate, and production amplitudes ${}^{k\epsilon}V_\alpha^\epsilon$ that we obtain by fitting,

$$\mathcal{I}(\tau) = \sum_{k\epsilon\epsilon'}\sum_{\alpha\alpha'}\epsilon\epsilon'\rho_{\epsilon\epsilon'}(\tau)^{k\epsilon'}V_{\alpha'}^{*\epsilon'}A_{\alpha'}^*(\tau)^{k\epsilon}V_\alpha^\epsilon A_\alpha(\tau) \tag{12}$$

where $\rho_{\epsilon\epsilon'}(\tau)$ is the beam spin-density matrix, ϵ and α enumerate the interfering amplitudes and k the non-interfering amplitudes.

The procedure then for decomposing the angular distribution of an $X \to I + B$ decay into partial waves is then:

- write down all possible spin-parities for the decay $X \to I + B$,
- write down the form for the decay amplitude for each spin-parity combination,
- for each event, calculate each decay amplitude and then vary the production amplitudes to maximize the likelihood of the event occurring,
- once the likelihood is maximized, write out the production amplitudes for each wave.

We typically perform our fits in bins of constant X mass, and vary the production amplitudes on an event-by-event basis to maximize the likelihood of the event occuring. As the amplitudes are complex numbers, we can plot the modulus (intensity) and the relative phase for each bin. If a resonance exists, it will show a peak in the intensity spectrum, and phase motion relative to a reference wave.

One of the most important steps in any partial wave analysis is the calculation of the decay amplitudes. The helicity formalism, developed by Jacob and Wick [28], calculates the decay amplitude of $X \rightarrow I + B$ by first considering all spin projections as eigenvalues of the helicity operator, which projects the spin along the direction of the momentum. This is convenient because the spin projection remains invariant save only for reflections, and in this regard it is convenient to transform to a basis where the helicity states are eigenstates of the reflection operator Y, defined as

$$Y = e^{i\pi J_y} P \tag{13}$$

$$Y\psi_{p,s} = \epsilon\psi_{p,-s} \tag{14}$$

where P is the parity operator, and ϵ is the *reflectivity*, the eigenvalue of the reflectivity operator. In this basis, a linear combination of decay amplitudes can be found which is an eigenstate of parity in the production process:

$$\mathcal{A}^a_{J,M}(\tau) = \Theta(M)\left[A^{J,M}_\alpha(\tau) - \epsilon P_X(-1)^{P-M}A^{J,-M}_\alpha(\tau)\right] \tag{15}$$

where $\Theta(M) = \frac{1}{\sqrt{2}}, \frac{1}{2}, 0$ for $M < 0, M = 0, M > 0$ respectively, and the amplitudes $A^{J,M}_\alpha$ are products of the decay amplitudes at each vertex in the decay chain,

$$A^{J,M}_\alpha(\tau) = A^{\lambda_1\lambda_2;M}_X \times A^{\nu_1\nu_2;\lambda}_I \times ... \tag{16}$$

where

$$A^{\lambda_1\lambda_2;M}_X = \mathcal{D}^J_{\lambda M}(\theta,\phi)\frac{\sqrt{L(L+1)}}{\sqrt{J(J+1)}}\langle L,0;S,\lambda|J,\lambda\rangle\langle S_1,\lambda_1;S_2-\lambda_2|S,\lambda\rangle K(\tau) \tag{17}$$

where $\mathcal{D}^J_{\lambda M}(\theta,\phi)$ are known as the Wigner "big-D" functions and $K(\tau)$ is usually a Breit-Wigner distribution.

Another technique for calculating amplitudes is commonly known as the Rarita-Schwinger [30] or Zemach [29] formalism. This procedure encodes a spin-J particle into a rank-J polarization tensor, and decay amplitudes are

written simply by forming a Lorentz scalar with the polarization tensor, decay momenta, the Levi-Civita tensor, and orbital angular momentum tensors.

The Rarita-Schwinger formalism has the advantage of being completely covariant–the helicity formalism requires boosting from decay vertex to decay vertex, which adds a bit of conceptual complexity. In addition, half-integer and integer spin states receive a uniform treatment in the Rarita-Schwinger formalism, which makes partial wave analyses of datasets containing both meson and baryon resonances much easier to handle than in the helicity formalism, where half-integer and integer spin states have different reflectivity bases. However, the Rarita-Schwinger formalism suffers in computational efficiency as the spins get larger–as spins increase in the helicity formalism, the additional complications are only the more complicated forms of the higher-order Wigner $\mathcal{D}^J_{\lambda M}$ and $d^J_{\lambda M}$ functions. As spins increase in the Rarita-Schwinger formalism, the ranks of the tensors increase, so that computing an amplitude for a spin-J state becomes a matter of multiplying rank-J tensors.

It is important to remember that we fit each mass bin independently, using an event-by-event maximum likelihood method. While this method is computationally expensive (fitting hundreds of thousands of events versus a few dozen data points) it is far more robust than χ^2 fitting because we impose no shape on the distribution; the underlying physics completely determines what we see. But, unlike χ^2 fitting, maximum likelihood fitting does not have an inherent "goodness-of-fit" parameter. This means that the procedure for determining whether one has reached the correct combination of partial waves for a given dataset is somewhat subjective. Typically, the procedure involves fitting the dataset with a large set of waves (a "complete" basis), which ought to give the best possible fit. Then different partial waves are turned on and off until a minimal set of waves producing a fit is obtained that is comparable with the complete-basis fit.

In any case, once the amplitudes are calculated and the fits performed, we generate a large set of Monte Carlo events uniformly over the phase-space of the system in question. We then feed these events through a simulation of the CLAS detector to correct for acceptance, and then we weight the accepted Monte Carlo by our fit results. We can then compared the weighted accepted Monte Carlo to our actual data, and if we have found a good fit, they should look identical.

2.1 Past Experimental Results

One of the first experiments to claim evidence for exotic mesons was the GAMS experiment, performed in 1988 at the Super Proton Synchrotron, located at CERN. The GAMS collaboration found that a fit containing the D_+, D_0

(both corresponding to the $a_2(1320)$ with $J^{PC} = 2^{++}$), and P_0 (corresponding to a new $J^{PC} = 1^{-+}$ exotic) partial waves described a sample of data in the $\pi^- p \to \eta\pi^0 n$ channel. The new 1^{-+} state was found to be centered at 1400 MeV/c^2, and the GAMS collaboration published a claim for the discovery of an exotic [14]. However, these results were later thrown into dispute when one of the GAMS collaborators later pointed out [15] that their fit did not take into account mathematical ambiguities arising from a spinless two-particle system, which in fact allow for up to eight different and equally valid solutions to the fit.

In 1993, the VES collaboration published results of a fit to a sample of data in the $\pi^- N \to \eta\pi^- N$ and $\pi^- N \to \eta'\pi^- N$ channels [16]. Their results showed a small, broad enhancement in the P_+ wave, which corresponds to a $J^{PC} = 1^{-+}$ wave in the natural parity exchange channel (whereas the GAMS result was in the unnatural parity exchange channel). However, the VES collaboration chose not to claim the observation as an exotic.

Later in 1993, a collaboration at KEK published results from a fit to a sample of $\pi^- p \to \eta\pi^- p$ data [17]. They too observed an enhancement in the 1400 MeV/c^{2}mass region in the P_+ wave, but they did not observe any phase motion relative to the $a_2(1320)$ D_+ wave. Therefore, they also did not claim a 1^{-+} resonance.

Finally, in 1997, the E852 collaboration at Brookhaven published the results of a fit to a data sample of $\pi^- p \to \eta\pi^- p$ [18], claiming the discovery of a 1^{-+} exotic at 1400 MeV/c^2. Their fits (including all eight ambiguous solutions, as GAMS did not) demonstrated the existence of a broad enhancement from 1200 to 1600 MeV/c^{2}in the P_+ partial wave, in addition to the dominant $a_2(1320)$. The relative phase motion between the a_2 and the 1^{-+} wave, now known as the $\pi_1(1400)$, also showed behavior beyond that of just a typical a_2 decay.

However, even though this claim was confirmed shortly after by the Crystal Barrel collaboration [25], the E852 $\pi_1(1400)$ claim was also not without controversy. Calculations using the flux-tube model [13] have placed the mass of the lightest 1^{-+} exotic at a minimum of 1800 MeV/c^2, uncomfortably far from the observed mass of the $\pi_1(1400)$. There have been several alternative explanations of the sightings of the $\pi_1(1400)$, including final-state interactions masquerading as a resonance [19] (much like the σ meson providing the intermediate-range attraction of the nucleon-nucleon potential), as well as the Deck effect and a resonance cusp effect. These discussions are ongoing; however, we expect our dataset to provide a significant opportunity to elucidate the identity of the $\pi_1(1400)$.

The E852 collaboration also published results of a fit to a sample of events in the $\pi^- p \to \pi^-\pi^-\pi^+ p$ channel. Their results found the expected $a_1(1260)$, $a_2(1320)$, and $\pi_2(1670)$ in the $\rho(770)\pi$ and $f_2(1270)\pi$ decay channels. In addition, they also found evidence of a new $J^{PC} = 1^{-+}$ state at 1.6 GeV/c^{2}in the $\rho(770)$ isobar decay chain [26]. The P_+, P_-, and P_0 partial waves showed enchancements in the 1.1 to 1.4 GeV/c^{2}and 1.6 to 1.7 GeV/c^{2}mass

regions. The P_+ wave also showed rapid phase movement in the 1.5 GeV/c^{2}to 1.7 GeV/c^{2}regions relative to all other natural parity-exchange waves, and based on these observations, the E852 collaboration claimed discovery of a new 1^{-+} exotic at 1600 MeV, the $\pi_1(1600)$. However, the E852 collaboration was unable to make any claim on the enhancement in the 1.1 to 1.4 GeV/c^{2}mass region, due to leakage effects from the $a_1(1260)$.

As the $\pi_1(1400)$ has had a rather controversial history, so has the $\pi_1(1600)$. After the publication of the analysis in [26], members of the E852 collaboration from Indiana University disputed the results, and finally split from the E852 collaboration proper. The IU-E852 collaboration, as they came to be known, published results of a partial-wave analysis of a larger 3π dataset that puts the earlier $\pi_1(1600)$ claims into dispute [27]. Their analysis reproduces the results in [26], and then goes on to claim that using a larger set of partial waves (35 waves in [27] versus 21 in [26]), the previously-seen exotic signal identified as the $\pi_1(1600)$ disappears in both reaction channels.

The IU-E852 collaboration concludes that the observation of the 1^{-+} enhancement at 1600 MeV is due to leakage from the non-exotic $\pi_2(1670)$ and $a_4(2040)$. While the analysis in [26] does note that leakage occurs from the $\pi_2(1670)$, the authors maintain that the leakage is only significant at masses below 1300 MeV.

In any event, these claims are clearly in need of further study. Thus, the focus of this prospectus is an analysis of the charged 3π system in photoproduction data on a hydrogen target, with the aim of confirming the sighting of the $\pi_1(1600)$ found by E852.

2.2 Current Experiments

As described above, the first generation of exotic meson search experiments used pion beams. However, recent theoretical work indicates that when a real photon is considered as a meson interacting with an exchange vector meson, ordinary and hybrid mesons could be produced in equal amounts [20]. In pion production, the exotic signal is suppressed by a factor of ten [21], [22], [23]. Thus recent proposals for exotic meson experiments have largely been based on photoproduction.

The flagship experiment among the new proposals is the GlueX experiment, proposed in 1998 in parallel with an energy upgrade to the CEBAF accelerator at Jefferson Lab. GlueX aims to be the definitive exotic meson discovery and spectroscopy experiment, with plans for a 9 GeV tagged photon beam and a custom-designed detector optimized for meson spectroscopy. However, unstable and delayed funding of the CEBAF upgrade have pushed back the GlueX commissioning until at least 2011. In the meantime, a series of experiments in Jefferson Lab's Hall B using the existing CEBAF Large Acceptance Spectrometer (CLAS) have shown some promising results.

The first of these was Jefferson Lab experiment E99-005, employing a 5.7 GeV photon beam on a hydrogen target, completed in 2001. E99-005 produced a dataset of XXXXXX events in the $\gamma p \to \pi^+\pi^+\pi^- n$ channel, which were analyzed by Nozar [24]. Their results showed no clear evidence for the $\pi_1(1600)$ observed at Brookhaven. A number of possiblities exist:

- the theoretical arguments that hybrids should be produced on an equal footing with ordinary mesons is incorrect,
- the $\pi_1(1600)$ may not be a gluonic hybrid but perhaps a tetraquark,
- the analysis was not sensitive enough to see the $\pi_1(1600)$.

However, one certainly cannot rule out the findings established in [26] on the basis of this analysis alone. For the purposes of this prospectus, we are assuming that the analysis described in [24] was too restrictive.

The issue in question is that of the copius baryon background produced by the running conditions (`g6c` and `g12` had almost identical running conditions in terms of acceptance). CLAS is optimized for baryon spectroscopy and thus its best acceptance is at large angles, which is ill-suited for peripheral production. The analysis described in [24] shows large amounts of Δ and Σ backgrounds, and their strategy is to perform a series of cuts to remove these events, which led to a sizeable reduction in their statistics. The goal of the proposed analysis is to include these baryonic events in the partial wave analysis and fit them as well as the meson events that we are interested in, rather than attempting to cut them out. In addition, experiment E04-005 has acquired ten times the statistics as `g6c`, and with this new analysis, we should have a definitive answer on whether there are exotics to be found in the charged 3π system in photoproduction.

In response to the E99-005 results, another proposal for similar running conditions but longer duration was submitted to the Jefferson Lab Program Advisory Committee in December of 2003. Experiment E04-005 was approved with an A rating, and became the point experiment of the `g12` run.

3 Jefferson Lab Experiment E04-005

3.1 Experimental Setup

Jefferson Lab experiment E04-005, nicknamed "HyCLAS", ran during with the `g12` rungroup from April to June 2008 in Jefferson Lab's Hall B. It employed a 5.71 GeV photon beam incident on a liquid hydrogen target.

The Continous Electron Beam Accelerator Facility is located at Jefferson Lab in Newport News, Virginia, USA. It consists of a 7/8-mile long "racetrack"-style electron accelerator, with two linear accelerators (linacs) along the straightaways and steering magnets at either end. Jefferson Lab was and remains a pioneer in superconducting radio-frequency (SRF) cavity technology, used to accelerate electrons to energies up to 6 GeV. The superconducting cavities offer no resistance to electrical current, which means there is none of the resistive heating found in traditional cavities. This allows for a continous flow of electrons through the accelerator, giving CEBAF a 100% duty factor.

The acceleration process begins when electrons are produced by two-nanosecond pulsed laser light incident on a gallium arsenide photocathode. These electrons are then accelerated to 45 MeV in the injector, and then fed into the accelerator proper. Each of the two linacs can provide 600 MeV of energy, and five sets of steering magnets allow for up to five passes around the racetrack before delivery to the halls via a beam switchyard.

Jefferson Lab currently has three experimental halls, A, B, and C, located at the west end of the accelerator.

For the g12 run, CEBAF provided 5.71 GeV electron beam to Hall B, which is turned into a tagged photon beam inside the hall. A photon-beam event in CLAS begins when the electron beam strikes a metal (for unpolarized photons) or diamond (for polarized photons) radiator, causing the electrons to emit bremstrahllung photons. Then, magnets bend the post-radiator electrons down into a momentum spectrometer (the "photon tagger"made up of 384 scintillation detectors ("E-counters"), which based on their placement give a measurement of the electron's remaining energy after brehmstrahllung. Subtracting this from the known beam energy, we have a measurement of the incoming photon energy. Non-interacting electrons are bent into a beam dump beyond the tagging spectrometer. In addition, another layer of 61 scintillation detectors ("T-counters") are placed below the E-counters to make timing measurements for event photon selection during analysis. The T-counters then can identify which 2 ns beam pulse an electron was a part of, and when this time is propogated back to the radiator, gives the proper event start time. Then this time is increased by the time it takes the photon to travel from the radiator to the event vertex, and then the measurements of the start counter and time-of-flight detectors take over.

The `g12` target consisted of a 45-cm-long vessel of liquid hydrogen, centered 90 cm upstream from the center of the CLAS detector. The photons interact with the target and the new particles produced emerge out of the target vessel and into the main detector.

For the `g12` run, the standard CLAS detector package was used. CLAS itself is divided axially into six sectors, like an orange. Combined, it consists of (in order of increasing distance from the target):

- **a start counter for event timing.** The start counter is made of 24 scintillator paddles, six for each sector,

Figure 1: The CEBAF accelerator as viewed from the air. The accelerator is beneath the roads tracing out a racetrack shape, and Halls C, B, and A (left to right) are visible at the bottom.

surrounding the g12 target. With a timing resolution of 400 ps, the start counter plays an important role in particle identification and background reduction.

- **a 5T torus magnet for bending charged particles.** The torus magnet is made of 6 lobes, spaced every 60°, and produces a magnetic field that under normal operation bends positively-charged particles away from the beamline and negatively-charged particles back into the beamline. This allows the drift chamber system to measure curved tracks, and the curvature of a charged particle's path through a magnetic field is proportional to its momentum. For g12 the torus was operated at 1930 amperes, half of its maximum current, as a balance between momentum resolution (maximized at high field) and acceptance for negative particles.

- **three sets of drift chambers for charged particle tracking and momentum measurement.** The drift chambers, as mentioned above, measure the trajectory of the particle through the torus field. The Region 1 drift chambers are located near to the target where the magnetic field is weak. The Region 2 chambers are interleaved with the torus lobes, where the magnetic field is strong, and the Region 3 chambers are farthest out, where the field is again weak. Their placement is designed to give a complete picture of a given track's behavior in and out of the magnetic field.

- **a time-of-flight wall for event timing.** The time-of-flight detector consists of 342 scintillator paddles placed in six arrays of 57, one for each sector. The time-of-flight is essential for particle identification, as an accurate time measurement from the start counter paired with the path length from the start counter to the time-of-flight provides the opportunity to calculate the velocity. When paired with the momentum measurement from the drift chambers, one can calculate the mass of the particle that produced the track, and make a guess about its identity.

More detail is provided in Figure 3.1.

In addition, each of these detectors requires calibration after every experimental run. Calibration constants include everything from physical positions of detectors to electronics settings to physical properties of detectors. The general procedure for calibration requires the calibrator to use custom software to produce specialized histograms. These histograms are then fit and the parameters are written to a MySQL database, which is accessed during reconstruction to produce accurate results.

In support of the g12 rungroup, I am calibrating the time-of-flight detector.

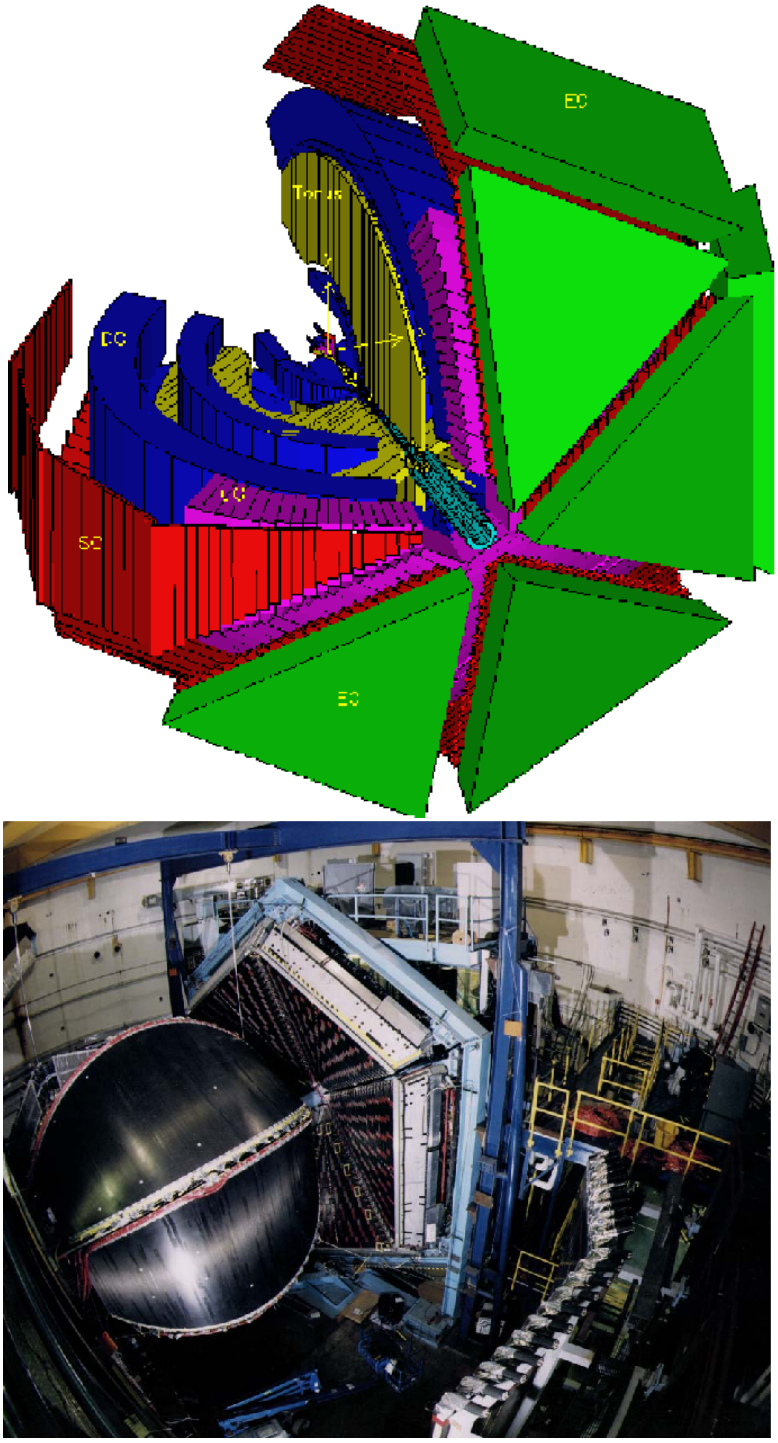

Figure 2: The CLAS detector as rendered in the GEANT detector simulation (left). A photo of CLAS ready for operation (right).

The process of calibrating the TOF is governed by the constants that need to be determined, namely (for photon runs):

- **counter status**: identify and eliminate dead channels,
- **ADC pedestals**: the readout of the ADCs when no tracks are passing through the TOF,
- **TDC linearization constants**: in the early years of CLAS operation, the TOF was instrumented with Fastbus TDCs that measured time nonlinearly–these constants were used to obtain the correct time from the TDC measurement. For the g12 run, the TOF was instrumented with new pipelined TDCs which are highly linear, so this calibration is largely unnecessary,
- **time-walk corrections**: an instrumental shift in the timing that occurs because the leading-edge discriminators currently in use cannot account for the finite rise-time of an ADC pulse,
- **left-right delay constants**: the relative time between the left and right photomultiplier tubes on the same scintillator paddle,
- **paddle to paddle offsets**: shifts in the relative timing between paddles due to cable lengths or other factors,
- **attenuation length**: the scintillation light created by the passage of a particle is attenuated by the time it reaches the photomultiplier tube, and this attenuation is related to how transparent the scintillator plastic is to light, which varies with age and usage,
- **effective velocity**: how fast light travels within the scintillator plastic, which can vary slightly with age and usage,
- **minimum-ionizing particle pulse heights**: the ADC readout for a particle passing through the scintillator with the minimum amount of energy needed to create a signal.

At present, the overall time resolution of the TOF for the `g12` run is about 300 picoseconds, with the goal being 200 picoseconds, which should be attained by the end of the summer of 2008.

Of these, XXXXX are consistent with three pion events. Within this sample, early cuts give us XXXXXX $\gamma p \to \pi^+\pi^+\pi^- n$ events.

4 Summary and Future Plans

Exotic meson spectroscopy has a rich and controversial history, and analyses of `g12` data stand to become the most authoritative voices in the debate. The 3π system has grown to be of especial interest with the results from E852, and the proposed analysis will be an important contribution to the understanding both of the spectroscopy of exotic mesons and the status of photoproduction as the preferred mode of production of exotics. While previous results have not been able to confirm the claims of E852, we hope that we have presented a compelling case for a thorough, high-statistics analysis of this channel.

This analysis will proceed as follows:

- complete calibrations and processing of the g12 dataset,
- establish and apply selection criteria for $\gamma p \to \pi^+\pi^+\pi^- n$ events,
- perform a rigorous partial wave analysis on our sample and identify all contributing resonances.

The preparation of the data for event selection and analysis will likely take until the spring of 2009. Partial-wave analysis being a computationally-expensive task, establishing the makeup of the 3π system in the g12 dataset is likely to take a year or more.

5 References

References

[1] M. Gell-Mann, Phys. Rev. **125**, 1067 (1962).

[2] V. E. Barnes *et al.*, Phys. Rev. Lett. **12**, 204 (1964).

[3] H. Fritzsch and M. Gell-Mann, eConf **C720906V2**, 135 (1972) [arXiv:hep-ph/0208010].

[4] S. L. Glashow, J. Iliopoulos and L. Maiani, Phys. Rev. D **2**, 1285 (1970).

[5] J. J. Aubert *et al.* [E598 Collaboration], Phys. Rev. Lett. **33**, 1404 (1974).

[6] J. E. Augustin *et al.* [SLAC-SP-017 Collaboration], Phys. Rev. Lett. **33**, 1406 (1974).

[7] J. L. Rosner, Phys. Rev. Lett. **21**, 950 (1968).

[8] A. Chodos, R. L. Jaffe, K. Johnson, C. B. Thorn and V. F. Weisskopf, Phys. Rev. D **9**, 3471 (1974).

[9] R. L. Jaffe, Phys. Rev. D **17**, 1444 (1978).

[10] T. Barnes, F. E. Close and S. Monaghan, Nucl. Phys. B **198**, 380 (1982).

[11] T. Barnes, F. E. Close, F. de Viron and J. Weyers, Nucl. Phys. B **224**, 241 (1983).

[12] N. Isgur and J. E. Paton, Phys. Rev. D **31**, 2910 (1985).

[13] T. Barnes, F. E. Close and E. S. Swanson, Phys. Rev. D **52**, 5242 (1995) [arXiv:hep-ph/9501405].

[14] D. Alde *et al.* [IHEP-Brussels-Los Alamos-Annecy(LAPP) Collaboration], Phys. Lett. B **205**, 397 (1988).

[15] Yu. D. Prokoshkin and S. A. Sadovsky, Phys. Atom. Nucl. **58**, 606 (1995) [Yad. Fiz. **58N4**, 662 (1995)].

[16] G. M. Beladidze *et al.* [VES Collaboration], Phys. Lett. B **313**, 276 (1993).

[17] H. Aoyagi *et al.*, Phys. Lett. B **314**, 246 (1993).

[18] D. R. Thompson *et al.* [E852 Collaboration], Phys. Rev. Lett. **79**, 1630 (1997) [arXiv:hep-ex/9705011].

[19] A. P. Szczepaniak, M. Swat, A. R. Dzierba and S. Teige, Phys. Rev. Lett. **91**, 092002 (2003) [arXiv:hep-ph/0304095].

[20] F. E. Close and P. R. Page, Phys. Rev. D **52**, 1706 (1995) [arXiv:hep-ph/9412301].

[21] F. E. Close and P. R. Page, Nucl. Phys. B **443**, 233 (1995) [arXiv:hep-ph/9411301].

[22] F. E. Close and J. J. Dudek, Phys. Rev. Lett. **91**, 142001 (2003) [arXiv:hep-ph/0304243].

[23] A. P. Szczepaniak and M. Swat, Phys. Lett. B **516**, 72 (2001) [arXiv:hep-ph/0105329].

[24] M. Nozar [CLAS Collaboration], arXiv:0805.4438 [hep-ex]. Under review for publication in Phys. Rev. Lett.

[25] A. Abele *et al.* [Crystal Barrel Collaboration], Phys. Lett. B **423**, 175 (1998).

[26] S. U. Chung *et al.*, Phys. Rev. D **65**, 072001 (2002).

[27] A. R. Dzierba *et al.*, Phys. Rev. D **73**, 072001 (2006) [arXiv:hep-ex/0510068].

[28] M. Jacob and G. C. Wick, Annals Phys. **7**, 404 (1959) [Annals Phys. **281**, 774 (2000)].

[29] C. Zemach, Phys. Rev. **133**, B1201 (1964).

[30] W. Rarita and J. S. Schwinger, Phys. Rev. **60**, 61 (1941).